

Received 21 September 2023, accepted 1 October 2023, date of publication 5 October 2023, date of current version 11 October 2023.

Digital Object Identifier 10.1109/ACCESS.2023.3322207



Discrete Time Signal Localization Accuracy in Gaussian Noise at Low Signal to Noise Ratios

CHRIS HALL[®] AND IVAN DJORDJEVIC[®], (Fellow, IEEE)
Electrical and Computer Engineering Department, The University of Arizona, Tucson, AZ 85721, USA

Corresponding author: Chris Hall (Chris93Hall@arizona.edu)

ABSTRACT Convolution and matched filtering are often used to detect a known signal in the presence of noise. The probability of detection and probability of missed detection are well known and widely used statistics. Oftentimes we are not only interested in the probability of detecting a signal but also accurately estimating when the signal occurred and the error statistics associated with that time measurement. Accurately representing the timing error is important for geolocation schemes, such as Time of Arrival (TOA) and Time Difference of Arrival (TDOA), as well as other applications. The Cramér Rao Lower Bound (CRLB) and other, tighter, bounds have been calculated for the error variance on Time of Arrival estimators. However, achieving these bounds requires an amount of interpolation be performed on the signal of interest that may be greater than computational constraints allow. Furthermore, at low Signal to Noise Ratios (SNRs), the probability distribution for the error is non-Gaussian and depends on the shape of the signal of interest. In this paper we introduce a method of characterizing the localization accuracy of the matched filtering operation when used to detect a discrete signal in Additive White Gaussian Noise (AWGN) without additional interpolation. The actual localization accuracy depends on the shape of the signal that is being detected. We develop a statistical method for analyzing the localization error probability mass function for arbitrary signal shapes at any SNR. Finally, we use our proposed analysis method to calculate the error probability mass functions for a few signals commonly used in detection scenarios. These illustrative results serve as examples of the kinds of statistical results that can be generated using our proposed method. The illustrative results demonstrate our method's unique ability to calculate the non-Gaussian, and signal shape dependent, error distribution at low Signal to Noise Ratios. The error variance calculated using the proposed method is shown to closely track simulation results, deviating from the Cramér Rao Lower Bound at low Signal to Noise Ratios.

INDEX TERMS Covariance matrices, delay estimation, digital measurements.

I. INTRODUCTION

Matched filtering is a frequently used signal processing technique. It is commonly used as a solution to two distinct classes of problems. The first class of problems is determining whether or not a specific signal occurred in a series of noisy sample measurements. This is known as the detection problem. Matched filtering for signal detection is well understood, with performance statistics documented in multiple textbooks [1], [2], [3]. This class of problems commonly pops up in communications systems and radar

The associate editor coordinating the review of this manuscript and approving it for publication was Jiafeng Xie.

signal processing [4], [5], [6]. The second class of problems is concerned with when a specific signal occurs. We will refer to this class of problems as the localization problem. Its solution is generally the time, or other x-axis variable, at which a peak in the matched filter output occurs. There are methods using interpolation which can estimate the time of arrival of the signal to within less than a sample period. There are also methods for handling cases involving interfering signals with known statistics. The analysis of error probabilities for the localization problem is not widely talked about or publicized in contrast to detection problem error statistics. Ronald Barker initially popularized this line of research in 1953 with his paper titled "Group synchronization of



Binary Digital Systems" by introducing Barker Codes which have correlation properties ideal for signal detection and localization [7]. Massey and others touched on the problem in the 1970s while researching maximum likelihood techniques for estimating the time of arrival of a known digital sequence in a larger digital sequence plus Gaussian noise [8]. In 1982 Stein published a paper defining the time of arrival error statistics for analog signals [9]. Stein's paper lacks a derivation, but remains the primary resource used when characterizing localization errors.

The localization problem is of critical importance in geolocation and remote sensing applications, where we are interested in calculating accurate error bounds on the location of a Radio Frequency (RF) emitter or receiver. In radar signal processing, localization error relates to the range resolution, which is an important performance metric. The localization problem also comes up in physical layer communications system design, where we must accurately locate the start of a physical layer frame in order to correctly demodulate the payload data. Research in this area has even been used to give insight into messenger RNA transcription processes that occur in cellular biology, where promoter regions must be accurately localized in order for the transcription process to be successful [10].

Remote sensing and geolocation systems translate Time of Arrival estimates into distance measurements using the known propagation speed of the transmitted signal. The error bounds on these measurements dictate the accuracy of the geolocation, and are typically translated into a 95% confidence ellipse centered on the geolocation estimate. This error ellipse is constructed using a calculated error variance and the assumption that the error is Gaussian. The error bounds are typically estimator error variances derived from the Cramér Rao Lower Bound for the continuous time signal case. It turns out that the Cramér Rao Lower Bound is a good bound for time of arrival estimator variance of high SNR continuous time signals. Other bounds, discussed later, have been successfully developed for cases where the SNR is lower. These methods were developed with continuous time signals in mind, but come with a claim that these bounds are also valid for discrete time signals if and only if you have the ability to interpolate by an undefined and sufficient amount. Furthermore, the assumption that the shape of the error distribution is Gaussian is only valid for the high SNR case, even on continuous time signals.

The work in this paper is motivated by a need to accurately characterize error statistics associated with signal Time of Arrival (TOA) estimates when the amount of interpolating used to perform the estimation is set at a fixed value or zero. The authors were unable to find work addressing this need in the current literature. The goal of this paper is to introduce a statistical model for the error distributions under the constraint of a discrete sampling interval, which is often true in real systems. This work will enable more accurate error bounds to be calculated for geolocations performed within the low SNR and discrete sampling constraint.

In section II we start by summarizing Stein's method which is commonly used to calculate localization error statistics. Then, in section III, we propose a new method for calculating localization errors in discrete time. The method we propose is derived directly from convolution fundamentals. Our work focuses on the specific scenario of a waveform in additive white Gaussian noise. We also address some practical considerations for evaluating the previously defined system. In section IV we discuss the boundary effects, how they distort our results, and how to compensate for them. Next, we briefly show how our model can be expanded to evaluate time difference of arrival errors in section V. Finally, in section VI we compare error probabilities for three common waveforms and present some illustrative results. Additional background on the matched filtering process is given in the appendix of this paper.

II. BACKGROUND

There are two publications that have addressed the signal localization accuracy problem in detail. Both publications focus on the continuous time solution, and arrive at similar results.

In "Algorithms for Ambiguity Function Processing," Seymour Stein states the following formula for calculating the standard deviation of Time Difference of Arrival (TDOA) measurements [9].

$$\sigma = \frac{1}{\beta} \frac{1}{\sqrt{BT\gamma}} \tag{1}$$

TDOA is a generalized case where two signals that have both been corrupted with noise are convolved with each other in order to estimate a relative time offset. This scenario typically occurs when we need to measure the time offset between the same signal received at two spatially diverse receivers in order to aid in the geolocating the emitter. B is the noise equivalent bandwidth at the receiver input, and is assumed to be the same for both receivers. β is the root mean squared (RMS) radian frequency defined by (2) and T is the signal duration. γ is the effective input SNR.

$$\beta = 2\pi \left[\frac{\int_{-\infty}^{\infty} f^2 W_s(f) df}{\int W_s(f) df} \right]^{\frac{1}{2}}$$
 (2)

 $W_s(f) = |x(f)|^2$ is the signal power spectral density, as shaped by the receiver and defined to have zero centroid.

The effective input SNR is defined by

$$\frac{1}{\gamma} = \frac{1}{2} \left[\frac{1}{\gamma_1} + \frac{1}{\gamma_2} + \frac{1}{\gamma_1 \gamma_2} \right] \tag{3}$$

where γ_1 and γ_2 are the SNRs for the respective receivers, within the noise equivalent bandwidth B.

The equation Stein introduced above is generalized for dealing with two noisy signals. He claims there is a 3 dB gain when one of the signals is clean. This should be directly derivable from (3). The shape of the distribution is not obvious, but, in practice, it is assumed to be Gaussian with zero mean.



Robert McDonough touches on the time of arrival problem in his book titled "Detection of Signals in Noise" on page 410 [11]. He establishes that this variance calculation introduced by Stein is the Cramér Rao Lower Bound (CRLB) for time of arrival estimation. Furthermore, it is easily achievable using any one of a variety of techniques, including convolution, provided there is sufficiently high SNR.

$$Var(\hat{\tau} - \tau) \ge \frac{1}{BT\beta^2\gamma}$$
 (4)

Stein and McDonough's work is with regard to continuous time signals. However, it has been shown to also be accurate for discrete time signals when adequate interpolation techniques are employed. This is the current state of the art for the vast majority of TOA error estimating systems.

The CRLB is a small error bound, and is not achievable for cases involving larger errors. The above formulas are said to hold true only at SNRs above 10dB, where there is low probability of spurious noise on the autocorrelation sidelobes exceeding a detection threshold [9]. Within this restriction, the errors in localizing the signal are due to output noise perturbations on the main lobe. Alternatives to the CRLB exist which provide a more accurate bound for the large error cases. The Barankin Bound and Ziv-Zakai Bound specifically have been used to calculate more accurate lower limits on the variance of time of arrival estimators in low SNR [12], [13], [14]. The Barankin Bound in particular, is the tightest bound possible on maximum likelihood estimators, and does converge to the CRLB at higher SNRs. The disadvantage with these methods is that they are difficult to calculate and have no closed form solution. However, some work has been done to approximate these bounds with piecewise functions of SNR under certain signal assumptions [13], [14]. As an example, (5) shows a piecewise approximation of the Ziv-Zakai bound on TOA estimator variance for narrowband signals [13].

$$\sigma^{2} = \begin{cases} D^{2}/12 & SNR \leq SNR_{1} \\ \frac{12\pi}{W^{3}TSNR} & SNR_{1} < SNR \leq SNR_{2} \\ Threshold & SNR_{2} < SNR \leq SNR_{3} \\ \frac{\pi}{WT\omega^{2}SNR} & SNR > SNR_{3} \end{cases}$$
 (5)

The specific SNR boundaries for each region and the variable definitions are explained in detail in the cited paper [13].

More recent research has been conducted with the goal of developing methods of estimation with errors approaching these lower bounds. Research in this area focuses on developing more sophisticated estimators, usually based on the simple correlation technique studied in this paper, which reduce error variance for a specific application or set of assumptions. The method of evaluation is repeated simulations with error variance being the only metric of interest [15], [16].

All of the methods mentioned above deal with estimating the time of arrival for continuous time signals or discrete time signals where there are no limits to the amount of interpolation we can perform on the signal. More significantly, these methods only give a lower bound on the variance of an estimator, and say nothing about what the error probability distributions may look like. In the rest of this paper we introduce a method of analysis which addresses both of these problems.

III. STATISTICAL MODEL

In this section we develop a statistical model to aid us in calculating the probability mass function for localization error in the presence of additive Gaussian noise. We define a jointly Gaussian system using two matrices: a Toeplitz matrix and a Difference matrix. Then, we integrate over a region of that probability density function to get the probability for a given index. We build a probability mass function by repeating this process for all indices in the valid range.

Before explaining the model, there are a few assumptions that we want to explicitly lay out. (1) We are limiting the range of possible peaks to the full region of convolution. (2) No interference signals are present. (3) Noise samples are Gaussian, zero-mean, independent, and identically distributed. (4) Potential peak values are restricted to integer index values. No interpolation between samples is utilized for peak finding. The model can easily be expanded in order to relax the last two constraints, as will be shown in more detail in future work.

A. TOEPLITZ MATRIX STRUCTURE

The purpose of the Toeplitz matrix is to model convolution with a filter. Here, H_T is the Toeplitz matrix and $h = [h_0, h_1, \dots, h_N]$ is the vector of filter taps which is the conjugate of the vector, x, in the case of matched filtering.

If our signal x has length N and our filter h is of length M, then the Toeplitz matrix should have dimensions N+M-1 by N+2M-2. The sequence, x, should be zero padded on both ends by M-1 so that its total length becomes N+2M-2. Then $y=H_Tx$ will be the expected full length of the convolution output, N+M-1.

Below is an example Toeplitx matrix, H_T , for the case where h is of length 3. A much larger Toeplitz matrix is depicted in Fig. 1.

$$\begin{bmatrix} h_0 & h_1 & h_2 & 0 & 0 & 0 & 0 \\ 0 & h_0 & h_1 & h_2 & 0 & 0 & 0 \\ 0 & 0 & h_0 & h_1 & h_2 & 0 & 0 \\ 0 & 0 & 0 & h_0 & h_1 & h_2 & 0 \\ 0 & 0 & 0 & 0 & h_0 & h_1 & h_2 \end{bmatrix}$$

$$(6)$$

The Toeplitz matrix can be used to calculate a convolution output, y, for an input vector, x.

$$y = H_T x \tag{7}$$

The output for a Gaussian noise vector input can be calculated in a similar manner. This defines a jointly Gaussian system.

$$n_T = H_T n \tag{8}$$

VOLUME 11, 2023 109597

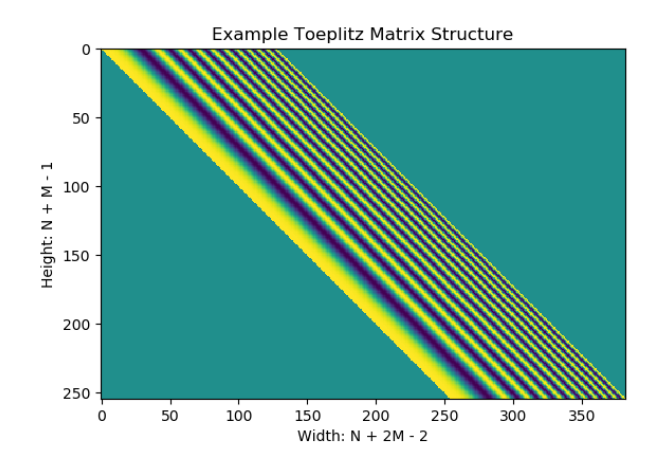


FIGURE 1. Example toeplitz matrix structure for a chirp signal.

The covariance matrix for this jointly Gaussian system is given as

$$C_1 = \sigma_n^2 H_T I H_T^T = \sigma_n^2 H_T H_T^T. \tag{9}$$

B. DIFFERENCE MATRIX STRUCTURE

The goal here is to measure the probability that one sample of the convolution output is greater than all of the other samples of the convolution output. To do this, we can generate a difference matrix as shown by (9).

$$H_D = \begin{bmatrix} -1 & 1 & 0 & 0 \\ -1 & 0 & 1 & 0 \\ -1 & 0 & 0 & 1 \end{bmatrix} \tag{10}$$

The dimensions of the difference matrix should be N + M - 2 by N + M - 1 where N is the length of x and M is the length of h. When we multiply our convolution output vector, y, by this difference matrix, H_D , the resulting vector is all negative if the sample in question is the peak. If not, then at least one element of the resulting vector will be positive.

Since this and the Toeplitz step are linear operations, we can define a jointly Gaussian distribution for the output vector by a covariance matrix and a mean vector, as shown in (10-12).

$$C_2 = H_D C_1 H_D^T = \sigma_n^2 H_D H_T H_T^T H_D^T$$
 (11)

$$\mu = H_D H_T x \tag{12}$$

$$p \sim \mathcal{N}(\mu, C_2) \tag{13}$$

Then, we integrate over a region of the probability density function to get a probability:

$$P = \int_{-\infty}^{0} \int_{-\infty}^{0} \cdots \int_{-\infty}^{0} p(x_1, x_2, \cdots, x_N) dx_1 dx_2 dx_N.$$
 (14)

P is the probability that sample zero of our convolution output is the peak. By doing a horizontal roll of the H_D matrix, we can evaluate the probability of other samples being the peak of the convolution output. Stepping through each of the roll increments will give us the complete Probability Mass Function for the convolution peak index.

Alan Genz discovered a computationally efficient numerical method for approximating integrals over these kinds of jointly Gaussian Probability Density Functions (PDFs) [17]. The Scipy python module contains a python wrapper around the original Fortran implementation of this method [18].

The function takes in arguments for the upper and lower bounds to integrate over. We want to integrate from minus infinity to zero. Since we can't actually provide negative infinity as a lower bound, we must choose a lower bound that is adequately small as to approximate negative infinity. We can accomplish this by iteratively testing lower and lower numbers until the difference in integration results becomes negligible. This works because we expect the tails of a jointly Gaussian distribution to tend towards zero.

Alternatively, Monte Carlo methods can give reasonable approximations as well. We found this to be slower than the Alan Genz method when implemented in Python. More sophisticated Monte Carlo methods and numerical approximation methods have recently been developed for calculating multivariate Gaussian probabilities, which could greatly improve the computation time, but these methods were not explored [19], [20].

For additive noise drawn from non-Gaussian distributions, the analysis can get a lot more complicated. In general, the weighted sum of two random variables does not have the same distribution as its parts. Although you can still carry out the calculations for the covariance matrix and the mean vector, the resulting distribution is not necessarily sufficiently defined by these two quantities.

Assuming the noise is drawn from a distribution which has well defined weighted sum properties, the model we have introduced can still work. Care must be taken to correctly propagate any additional distribution parameters through the linear system. Then Monte-Carlo methods would probably need to be used in order to integrate over the resulting Probability Density Function.

IV. BOUNDARY EFFECTS

When we calculate the full convolution, we encounter boundary effects. The probability of an index at the edges being the peak is artificially high compared to the rest of the signal. In fact, if we only feed zero mean Gaussian noise vectors as signals into the system, we still encounter these edge effects where we would expect every index to be equally probable.

The cause of these edge effects stems from the fact that every time we advance the convolution window, most of the signal samples do not change. This has an averaging effect where if one signal sample makes a correlation index particularly strong then the neighboring correlation indices will also be strong. The peak index probability gets spread across these neighboring correlation indices. The extent of the spreading is dependent on the filter length.



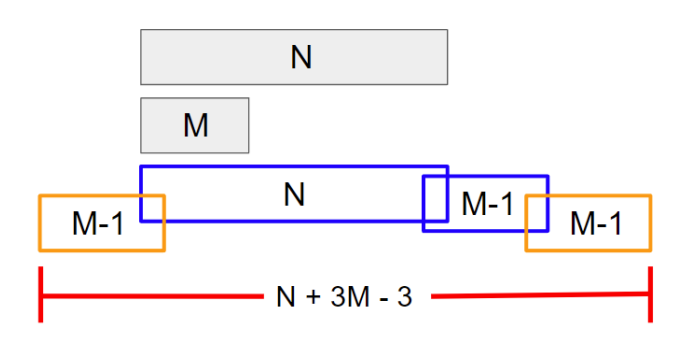


FIGURE 2. Extended convolution size to remove boundary effects.

At the boundaries of the convolved sequence this phenomenon cannot occur to the same extent. The probabilities can only be spread across the indices on one side, and this results in artificially high probabilities at the edges of the convolution range.

Technically these results are correct for the constraints we have set for ourselves. But these high edge probabilities would not exist if the signal to be detected existed within a longer noise vector, as is typically the case.

We can calculate the true peak index probability mass function without edge effects by applying our previously described method over an extended region, as shown in Fig. 2. This region will still have the edge effects, but they will be outside of the subregion we actually care about. Then we can pick out the subregion and normalize it to sum to one. The new shape of our Toeplitz matrix will be N + 3M - 3 by N + 4M - 4 and the dimensions of the difference matrix will be N + 3M - 4 by N + 3M - 3.

For the remainder of this paper our results will be calculated using this extension technique to remove edge effects.

V. TIME DIFFERENCE OF ARRIVAL

Measuring the Time Difference of Arrival (TDOA) of two signals generally means convolving two noisy signals with each other in order to estimate their relative time offset.

$$(s_1 + n_1) * (s_2 + n_2)$$

= $(s_1 * s_2) + (s_1 * n_2) + (s_2 * n_1) + (n_1 * n_2)$ (15)

The first term above is deterministic. The middle two terms are jointly Gaussian. The last term is not jointly Gaussian but also not dependent on the input signal at all. The statistics for this term are constant across the valid convolution region, so we can ignore it completely. The jointly Gaussian system generated from the middle two terms can be described as

$$y = H_D \begin{bmatrix} H_{T1} & H_{T2} \end{bmatrix} \begin{bmatrix} S_2 \\ S_1 \end{bmatrix}$$
 (16)

where H_{T1} and H_{T2} are the Toeplitz matrices generated from the signals S_1 and S_2 respectively. The two Toeplitz matrices are concatenated together as shown in the equation above. If S_1 and S_2 are of different lengths, the longer sequence

dictates the size for both Toeplitz matrices and the amount of zero padding required on both sequences.

The mean, μ , of the system is calculated by replacing the right hand term with

$$\begin{bmatrix} S_2 \\ 0 \end{bmatrix} \tag{17}$$

which yields the convolution term $(S_1 * S_2)$. The covariance matrix can then be calculated in the same way as before.

VI. ILLUSTRATIVE RESULTS

In this section we provide examples demonstrating the kinds of metrics our proposed analytical method can produce. We have purposely selected our results in order to clearly demonstrate the non-Gaussian nature of the time of arrival error distribution as well as the strong dependence on signal shape and filter shape when SNR is low. These features are not considered in prior research which deals almost exclusively in high SNR cases where these effects are negligible.

We have chosen three signal waveforms and calculated their localization error statistics using the methods we proposed and discussed above. Fig. 3 shows the three waveforms. The first waveform is a boxcar, chosen for its simplicity and popularity as a test signal. The second waveform is the length 13 Barker Code. Barker Codes are engineered to have a max autocorrelation sidelobe value of 1, making them ideal for localization tasks. The third waveform is a linear chirp, which sweeps through the full range of digital frequencies from 0 to π and is 128 samples long.

Fig. 4 shows the autocorrelation functions for each of the three test signals. The autocorrelation of a waveform gives us a general idea of how well we will be able to localize the signal using a matched filter. An ideal signal for localization will have an autocorrelation function with a strong center peak and low sidelobes. In the presence of noise, those sidelobes pose a risk of rising above the center peak and inducing localization errors. Therefor we want the sidelibe levels to be low relative to the center peak in order to reduce the probability of such errors occurring.

Figs. 5 through 7 show the time of arrival estimator error Probability Mass Functions for each of the test signals.

Fig. 8 shows the estimator variance with respect to SNR for a length 20 boxcar. Both the simulation and model results are compared against Stein's method, which represents the Cramér Rao Lower Bound (CRLB) [9]. At very low SNR the estimator variance approaches a limit at the variance of a uniform distribution, $\frac{n^2-1}{12}$, over the valid region we have defined. Stein's equation does not make the same valid region assumption and therefore does not have an artificial upper limit on the variance. It is necessary to emphasize that Stein's equation and other lower bounds mentioned previously are for a slightly different problem with a different set of assumptions and therefore are not directly comparable to our results. We have included this result purely for the sake of emphasizing those differences.

VOLUME 11, 2023 109599

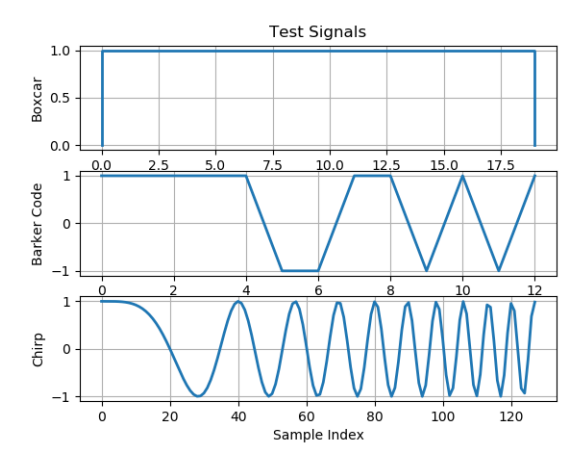


FIGURE 3. Three test signals: (a) Boxcar (b) Barker code (c) Chirp.

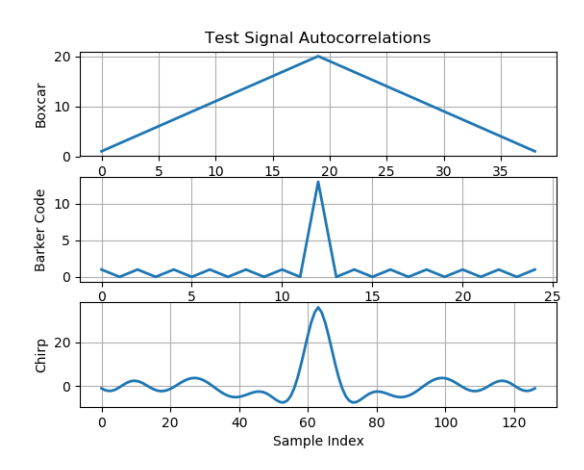


FIGURE 4. Autocorrelation functions for the three test signals: (a) Boxcar (b) Barker code (c) Chirp.

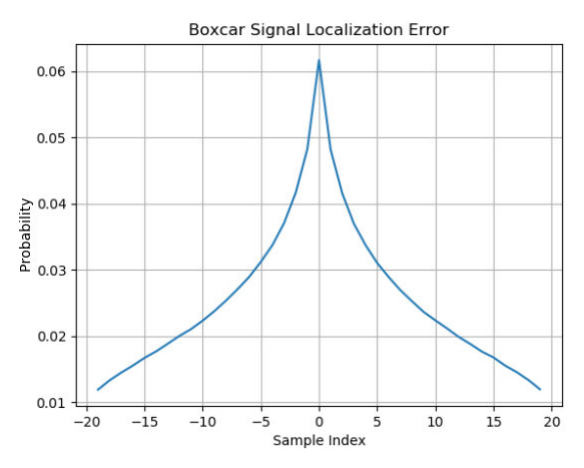


FIGURE 5. Boxcar length 20 at -15 dB SNR.

At higher SNR, the variance from our method closely tracks the CRLB and then dips down below the CRLB to zero. In this high SNR region, the noise will effectively never be able to add up enough to force an error of even one whole sample. In continuous time, the error continually decreases and can be calculated well below an assumed sample period. At lower SNR there is a significant gap between the CRLB,

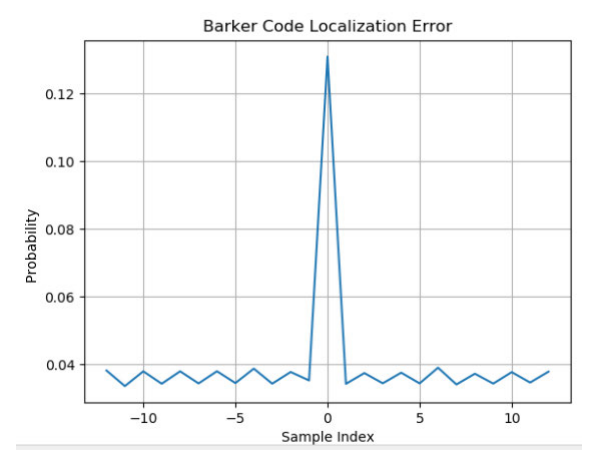


FIGURE 6. Length 13 Barker Code at -15 dB SNR.

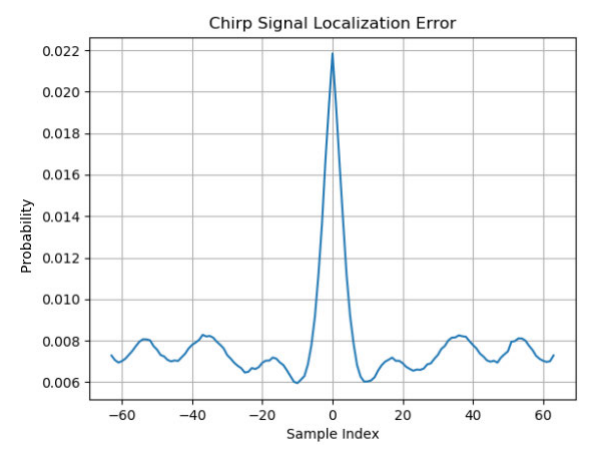


FIGURE 7. Length 64 chirp signal at -25 dB SNR.

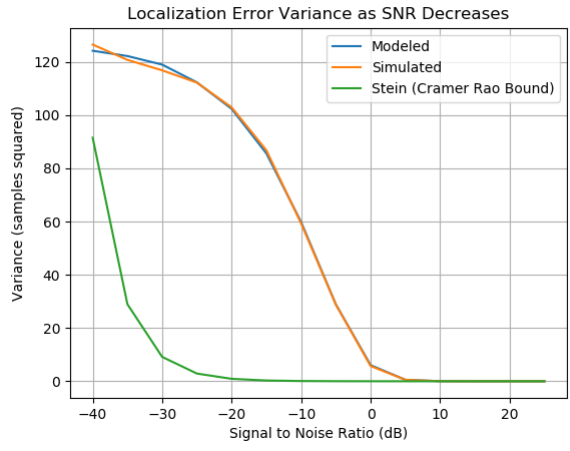


FIGURE 8. Estimator variance for a length 20 boxcar.

given by Stein's equation, and the time of arrival estimator variance given by our model.

When we attempt to localize a signal using a mismatched filter, we can get some interesting effects as shown in Fig. 9. The center of the convolution region has depressed probabilities due to the cross correlations between each sample and its neighbors. The elevated peaks in the Probability Mass Function occur at indices which also experience this cross correlation, but their neighboring indices don't compete



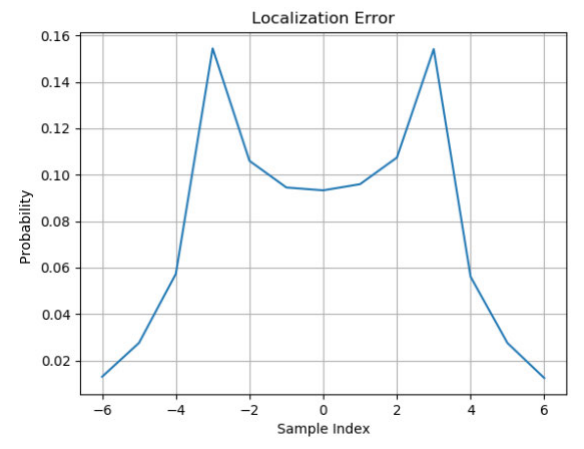


FIGURE 9. Length 4 boxcar and length 10 boxcar convolution at 0 dB SNR.

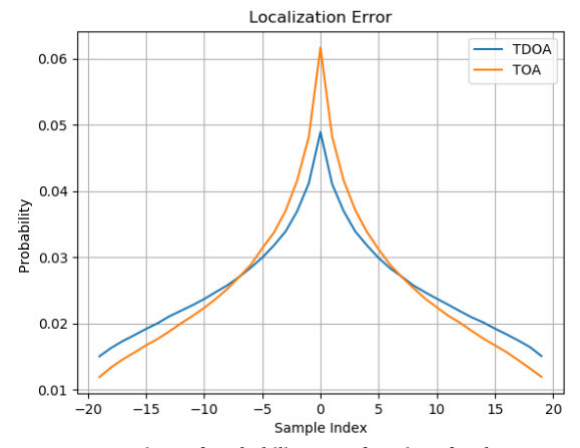


FIGURE 10. Comparison of probability mass functions for the TDOA and TOA scenarios for a length 20 boxcar at -15 dB.

as much because the shorter signal's window is falling off the edge of the longer signal. This effect is similar to the boundary effects described in section IV, but in this case they would still occur even if the signal existed within an infinitely long noise vector.

Fig. 10 shows how the error distributions can differ between the TOA scenario and TDOA scenario, for the same signal shape. Convolving two noisy signals will always result in a more error prone peak estimate, and higher estimator variance, than convolving a noisy signal with a clean template. However, no major differences in the general shape of the error distribution exist between the two cases.

VII. CONCLUSION

In this paper, we explored methods for calculating the statistics of localization errors when using convolution to detect a discrete time signal in Gaussian noise. We introduced Stein's equations which are the current preferred method for calculating the error variance. Stein's methods are great when iterative interpolation methods can be employed and if the SNR is sufficiently high, but do not hold true otherwise. At low SNRs, the localization statistics become heavily dependent on the shape of the detected signal and the shape of the filter.

We developed a linear model for the difference between any one signal autocorrelation index and all other autocorrelation indices. We used that model to define a jointly Gaussian system [21]. Using existing numerical integration methods, we were able to calculate the probability that any one convolution index is the peak output [17]. We then developed an extended method for calculating the same statistics in the case where both the detected signal and the filter have Gaussian noise added to them, as is true when taking TDOA measurements.

Lastly, we showed some examples of Probability Mass Functions for localization error. These plots were generated for three commonly used signal types: a boxcar, a barker code, and a chirp signal. These plots clearly show that the localization error is not Gaussian and depends on the shape of our signal of interest.

The posted results are for a case where the signals are critically sampled and not interpolated, such that the additive noise is independent and identically distributed. Oversampling or interpolation of the signal can be taken into account at the beginning of the introduced model. After all, an interpolated signal is just another signal. However, care must be taken to incorporate the true noise covariance matrix at the start of the model. The assumption of independent and identically distributed noise would no longer hold true in this case.

The methods presented in this paper are directly applicable to TOA and TDOA geolocation as well as remote sensing in general. The current prevailing method of generating error probability bounds is to calculate a 95 percent certainty ellipse based on error that is Gaussian distribed and variance given by Stein's equation, irrespective of the shape of the signal to be detected.

The approach we have taken in this research is unique because we are not simply trying to calculate a tighter lower bound on Time of Arrival estimator variance. Instead we focus on the actual estimator variance and distribution for a specific, but very common, case in which the previously published lower bound methods do not apply. The distinguishing characteristic of the case we have outlined is a limited ability to interpolate the given signal when peak finding. Additionally, our proposed model allows us to calculate a probability distribution for the error in addition to the error variance, which is not available using previously discussed lower bound methods. These probability distributions are particularly interesting at low SNRs, as shown in our illustrative results. The introduced method enables the calculation of more well defined error bounds on geolocations of low SNR signals.

APPENDIX A CONVOLUTION AND MATCHED FILTERING

The convolution operation is defined by the following equation.

$$y[\tau] = \sum x[n]h[\tau - n] \tag{18}$$

VOLUME 11, 2023 109601



If $h[n] = x^*[\tau - n]$ then h[n] is a matched filter. Matched filtering is a common technique for detecting complex signals as well as purely real signals. It is the optimal signal detection method for a known and deterministic signal in Additive White Gaussian Noise (AWGN).

It is common practice to normalize the filter, h[n], to have unit energy. This is done by muliplying h[n] by a constant $\frac{1}{\sqrt{E_h}}$ where $E_h = \sum h^2[n]$. If we are filtering additive white Gaussian noise, the output will be Gaussian noise of the same power as the input.

We will be assuming all signals are digital and critically sampled such that the additive Gaussian noise samples are uncorrelated.

$$\sigma^2 = var\left(\sum h[n]\sigma_n^2\right) = \sigma_n^2 \sum h^2[n]$$
 (19)

where $\sum h^2[n] = 1$

The output of the matched filter at a time when its matched signal occurs is as follows:

$$y = \sum x[n] * h[n] = (x_0 h_0 + x_1 h_1 + \dots)$$
 (20)

$$=\frac{1}{\sqrt{E_r}}\sum x^2[n] \tag{21}$$

The power of the output at that instant, y^2 , would then be E_x . This gives us a Signal to Noise Ratio (SNR) at the output of the matched filter of $\frac{E_x}{\sigma_n^2}$ at the time when the matched signal is present. It can be shown that this SNR result holds true even when the matched filter is not normalized to unit energy.

REFERENCES

- S. M. Kay, Fundamentals of Statistical Signal Processing: Detection Theory. Upper Saddle River, NJ, USA: Prentice-Hall, 1993.
- [2] L. L. Scharf, Statistical Signal Processing: Detection, Estimation, and Time Series Analysis. Reading, MA, USA: Addison-Wesley, 1991.
- [3] A. V. Oppenheim and R. W. Schafer, Discrete-Time Signal Processing, 3rd ed. Upper Saddle River, NJ, USA: Prentice-Hall, 2009.
- [4] J. G. Proakis, *Digital Communications*, 5th ed. New York, NY, USA: McGraw-Hill, 2007.
- [5] M. A. Richards, Fundamentals of Radar Signal Processing. New York, NY, USA: McGraw-Hill, 2005.
- [6] M. I. Skolnik, Radar Handbook. New York, NY, USA: McGraw-Hill, 1970.
- [7] R. H. Barker, "Group synchronizing of binary digital systems," *Commun. Theory*, pp. 273–287, Sep. 1952.
- [8] J. Massey, "Optimum frame synchronization," IEEE Trans. Commun., vol. COM-20, no. 2, pp. 115–119, Apr. 1972.
- [9] S. Stein, "Algorithms for ambiguity function processing," *IEEE Trans. Acoust., Speech, Signal Process.*, vol. ASSP-29, no. 3, pp. 588–599, Jun 1981
- [10] J. Weindl and J. Hagenauer, "Applying techniques from frame synchronization for biological sequence analysis," in *Proc. IEEE Int. Conf. Commun.*, Jun. 2007, pp. 833–838.
- [11] R. McDonough and A. Whalen, Detection of Signals in Noise. Amsterdam, The Netherlands: Elsevier, 1995.
- [12] A. Zeira and P. M. Schultheiss, "Realizable lower bounds for time delay estimation," *IEEE Trans. Signal Process.*, vol. 41, no. 11, pp. 3102–3113, Nov. 1993.
- [13] A. Weiss and E. Weinstein, "Fundamental limitations in passive time delay estimation—Part I: Narrow-band systems," *IEEE Trans. Acoust., Speech, Signal Process.*, vol. ASSP-31, no. 2, pp. 472–486, Apr. 1983.
- [14] E. Weinstein and A. Weiss, "Fundamental limitations in passive time-delay estimation—Part II: Wide-band systems," *IEEE Trans. Acoust., Speech, Signal Process.*, vol. ASSP-32, no. 5, pp. 1064–1078, Oct. 1984.

- [15] Y. Li, Q. Ma, B. Wang, M. Dong, L. Zhang, and J. Peng, "Time delay estimation algorithm of partial discharge ultrasound signal based on wavelet transform image convolution," in *Proc. IEEE Conf. Electr. Insul. Dielectr. Phenomena (CEIDP)*, Oct. 2022, pp. 310–315.
- [16] R. Hanus, M. Zych, R. Chorzępa, and A. Golijanek-Jędrzejczyk, "Investigations of the methods of time delay measurement of stochastic signals using cross-correlation with the Hilbert transform," in *Proc. IEEE* 20th Medit. Electrotechn. Conf. (MELECON), Jun. 2020, pp. 238–242.
- [17] A. Genz, "Numerical computation of multivariate normal probabilities," J. Comput. Graph. Statist., vol. 1, no. 2, pp. 141–149, Jun. 1992.
- [18] P. Virtanen et al., "SciPy 1.0: Fundamental algorithms for scientific computing in Python," *Nature Methods*, vol. 17, pp. 261–272, Mar. 2020.
- [19] D. Frisch and U. D. Hanebeck, "Efficient deterministic conditional sampling of multivariate Gaussian densities," in *Proc. IEEE Int. Conf. Multisensor Fusion Integr. Intell. Syst. (MFI)*, Sep. 2020, pp. 75–81.
- [20] Z. Botev, D. Mackinlay, and Y.-L. Chen, "Logarithmically efficient estimation of the tail of the multivariate normal distribution," in *Proc. Winter Simulation Conf. (WSC)*, Dec. 2017, pp. 1903–1913.
- [21] S. M. Kay, Fundamentals of Statistical Signal Processing: Estimation Theory. Upper Saddle River, NJ, USA: Prentice-Hall, 1993.



CHRIS HALL received the B.S. degree in electrical engineering and computer engineering from George Mason University, in 2016, and the M.S. degree in electrical engineering from the University of Wisconsin–Madison, in 2017. He is currently pursuing the Ph.D. degree in electrical engineering from The University of Arizona. He is an Engineer with Rincon Research Corporation, Tucson, AZ, USA.



IVAN DJORDJEVIC (Fellow, IEEE) received the Ph.D. degree from the Faculty of Electronic Engineering, University of Nis, in 1999.

He is currently a Professor of electrical and computer engineering and optical sciences with The University of Arizona, Tucson, AZ, USA, and the Director of the Optical Communications Systems Laboratory and the Quantum Communications Laboratory. Before joining The University of Arizona, he held appointments with the University

sity of Bristol, U.K.; the University of the West of England, U.K.; Tyco Telecommunications, USA; the National Technical University of Athens, Greece; and State Telecommunication Company, Niš, Yugoslavia. He has authored/coauthored 11 books, 13 book chapters, more than 580 journal and conference publications, and he holds 55 U.S. patents.

Dr. Djordjevic is a fellow of the Optica (formerly OSA). He has served as an Associate Editor for *Journal of Optical Communications and Networking*, from 2019 to 2023. From 2012 to 2021, he was an Area Editor/a Senior Editor/an Editor of IEEE Communications Letters. From 2016 to 2021, he was an Associate Editor/Editorial Board Member for both *Journal of Optics* (IOP) and *Physical Communication* (Elsevier). He has been serving as an Editor for IEEE Transactions on Communications, *Optical and Quantum Electronics*, and *Frequenz*.